BBA - Molecular Basis of Disease 1870 (2024) 167334

Contents lists available at ScienceDirect

BBA - Molecular Basis of Disease

journal homepage: www.elsevier.com/locate/bbadis

Peroxiredoxin 4 deficiency induces accelerated ovarian aging through destroyed proteostasis in granulosa cells

Xiaofei Zou [1], Xiuru Liang [1], Wangjuan Dai [1], Ting Zhu, Chaoyi Wang, Yutian Zhou, Yi Qian, Zhengjie Yan, Chao Gao, Li Gao, Yugui Cui, Jiayin Liu, Yan Meng [*]

State Key Laboratory of Reproductive Medicine and Offspring Health, Clinical Center of Reproductive Medicine, the First Affiliated Hospital of Nanjing Medical University, Nanjing, Jiangsu Province, China

ARTICLE INFO

Keywords:
Peroxiredoxin 4 (PRDX4)
Ovarian aging
Protein homeostasis
Granulosa cells
Oxidative protein folding
Follicle-stimulating hormone receptor (FSHR)

ABSTRACT

Ovarian aging, a complex and challenging concern within the realm of reproductive medicine, is associated with reduced fertility, menopausal symptoms and long-term health risks. Our previous investigation revealed a correlation between Peroxiredoxin 4 (PRDX4) and human ovarian aging. The purpose of this research was to substantiate the protective role of PRDX4 against ovarian aging and elucidate the underlying molecular mechanism in mice. In this study, a *Prdx4*$^{-/-}$ mouse model was established and it was observed that the deficiency of PRDX4 led to only an accelerated decline of ovarian function in comparison to wild-type (*WT)* mice. The impaired ovarian function observed in this study can be attributed to an imbalance in protein homeostasis, an exacerbation of endoplasmic reticulum stress (ER stress), and ultimately an increase in apoptosis of granulosa cells. Furthermore, our research reveals a noteworthy decline in the expression of Follicle-stimulating hormone receptor (FSHR) in aging *Prdx4*$^{-/-}$ mice, especially the functional trimer, due to impaired disulfide bond formation. Contrarily, the overexpression of PRDX4 facilitated the maintenance of protein homeostasis, mitigated ER stress, and consequently elevated E2 levels in a simulated KGN cell aging model. Additionally, the overexpression of PRDX4 restored the expression of the correct spatial conformation of FSHR, the functional trimer. In summary, our research reveals the significant contribution of PRDX4 in delaying ovarian aging, presenting a novel and promising therapeutic target for ovarian aging from the perspective of endoplasmic reticulum protein homeostasis.

1. Introduction

Ovary is the most important female reproductive organ, which can produce oocytes and secrete sex hormones to maintain female fertility and endocrine homeostasis [1]. It is the first organ to show signs of physiological aging and the ovarian function declines significantly after 30 years old [2]. During ovary aging, follicle number and oocyte quality decreases, which leads to a decline in fertility and an increase in the incidence of various pregnancy complications and offspring health issues [3]. Differing from general public belief, assisted reproductive techniques cannot efficiently circumvent age-related fertility problems [4]. Due to the increasing number of pregnant women with advanced maternal age, it is urgent to find therapeutic targets for diminished ovarian reserve. Clinically, ovarian aging has been associated with other disorders, such as hot flashes, sweating, sleep disorders, vaginal dryness, depression, and mental health problems [5]. Therefore, giving further insights into the underlying mechanisms of ovarian aging is critical to identify effective preventions and therapies for those clinical symptoms.

Both genetic and environmental factors contribute to ovarian aging, and there is an inter-individual variability in these age-related changes [6]. Aging-related quality decline in granulosa cells surrounding the oocyte is one of the most important biological events for ovarian aging [7]. Numerous studies have solidified the significant role of granulosa cells as an indicator of the aging ovary. Granulosa cells not only play an essential role in synthesizing steroid hormones but also in follicle development because they provide nutrients and mechanical support through physical interactions for oocytes [8]. In addition to oxidative stress, advanced glycation end products, DNA damage, mitochondrial and protein dysfunction, telomere shortening, proinflammatory cytokine and inflammation, the molecular basis of ovarian aging is

* Corresponding author.
E-mail address: ctmengyan@njmu.edu.cn (Y. Meng).
[1] These authors contributed to the work equally and should be regarded as co-first authors.

https://doi.org/10.1016/j.bbadis.2024.167334
Received 29 February 2024; Received in revised form 24 June 2024; Accepted 27 June 2024
Available online 5 July 2024

multifactorial and not fully known [9]. Loss of proteostasis is one of the hallmarks of many age-associated diseases [10] which represents common denominators of aging in different organisms [11,12] while little in the study of ovarian aging, so it becomes a new perspective to find the potential diagnostic biomarker and therapeutic target for diminished ovarian reserve.

Peroxiredoxin 4 (PRDX4), a protein located in the endoplasmic reticulum (ER), is involved in enhancing the efficiency of oxidative protein folding, thereby assuming a pivotal function in maintaining protein homeostasis [13]. Our previous data showed that PRDX4, which is located in the granulosa cells, is related to human ovarian aging because the expression level is significantly lower in premenopausal women's ovary than young women's [14]. We also confirmed that PRDX4 can protect mice from ovarian aging in the condition of D-gal-induced oxidative damage [15]. There was also a study suggesting that human granulosa cells exhibited aging-associated downregulation of PRDX4 [16], so PRDX4 was regarded to have an ameliorating effect on ovarian aging and female age-related fertility decline.

PRDX4, which is essential for enzymatic oxidative protein folding [17] to obtain the correct spatial conformation of the protein, has been confirmed to catalyze the formation of disulfide bonds in some hydrogen peroxide-mediated nascent protein synthesis together with ER-resident protein disulfide isomerase (PDI) family proteins [18]. The intramolecular disulfide bonds contribute significantly to both the folding process and the overall structural stability of proteins [19,20]. PRDX4 is well positioned to use H_2O_2 produced by ER oxidoreductase 1 (ERO1), to generate another pair of disulfide bonds, and so enhancing the efficiency of oxidative protein folding [13]. Therefore, PRDX4 is relevant to the occurrence and prognosis of many diseases. For example, PRDX4 driven oxidative protein folding is associated with final functional proteogenesis such as proinsulin folding [21]. B- to plasma-cell differentiation is characterized by a massive expansion of the ER, finally sustaining abundant disulfide-rich immunoglobulin (Ig) synthesis and secretion. In the absence of PRDX4, the process of IgM polymerization and quality control are impaired, which results in enough native Polymers secreted but more transport-incompetent aberrant IgM accumulation and then ER stress occurred [22]. The deficiency of PRDX4 and ERO1 affect the synthesis of collagen, which causes ascorbic acid depletion [23]. Whether PRDX4 will regulate the correct spatial conformation of important proteins in granulosa cells and thus affect ovarian function have not been studied yet.

To be properly oxidative folded in the ER is crucially important for the newly synthesized protein [24], therefore it is crucial for protein homeostasis. Follicle-stimulating hormone receptor (*Fshr*) gene is one of the important genes associated with primary ovarian insufficiency, which is mainly expressed in the granulosa cells of developing follicles in the ovary at high expression level [25]. Follicle-stimulating hormone receptor (FSHR) is rich in disulfide bonds, and oxidative folding is especially important for its fuction [26]. Furthermore, it has been substantiated that FSHR exists as a functional trimer. Additionally, the enigmatic hinge region, which is part of the integral structure of the entire extracellular domain of FSHR, contains two peculiar sequence motifs coupled by three disulfide bonds [27,28]. The links by these disulfide bonds ensure an integrated and stable conformation of the FSHR structure [29]. However, the role of unusual FSHR conformation in ovarian aging is rarely reported. We speculated that PRDX4, a protein implicated in augmenting the efficacy of oxidative protein folding in the ER, may uphold protein homeostasis, suppress ER stress, and thereby sustain the functionality of ovarian granulosa cells, thus playing a protective role in ovarian function. The accumulation of unusual conformation FSHR may exist in granulosa cells due to PRDX4 deficiency and become one of the important factors exacerbating ovarian aging process.

In this research, we studied the fertility related indicators of *Prdx4* knockout mice aged 4–12 months to confirm whether PRDX4 deficiency could induce accelerated ovarian aging and the related mechanisms. We also established *Prdx4* knockdown and overexpression KGN cells to further study the underlying molecular mechanisms of these phenomena. We found that the accelerated decline in ovarian function is due to the destroyed proteostasis in the granulosa cells , and then led to exacerbated ER stress and increased apoptosis of granulosa cells. The most notable discovery was that the deficiency of PRDX4 significantly compromised the expression of FSHR, especially the functional trimer, in aging *Prdx4*$^{-/-}$ mice, which is one of the major genes protecting the ovary function and is abundantly expressed in the granulosa cells.

2. Methods

2.1. Animal care

C57BL/6J mice were obtained from the Nanjing Biomedical Research Institute of Nanjing University, Nanjing, China. The mice were kept in regulated environments with access to water and food. They were housed under standard conditions , maintaining controlled temperatures (21–25 °C), humidity levels (40 % - 70 %) , and a light-dark cycle from 7 a.m. to 7 p.m. The experimental procedures were approved by the Regional Ethical Committee of Nanjing Medical University and conducted according to the guidelines of the ACUC of Nanjing Medical University School of Medicine Laboratory Animal Research Center (IACUC - 1711029).

2.2. Generation of mice

In this study, female C57BL/6J mice were obtained from the Nanjing Biomedical Research Institute of Nanjing University (Nanjing, China). Young (4 months) and aging (9 months) female C57BL/6J mice were divided into two groups of five mice each: the wild-type(*WT)* and *Prdx4* knockout (*Prdx4*$^{-/-}$) groups, respectively. *Prdx4*$^{-/-}$ mice were generated using CRISPR/Cas9 as previously described [15]. Two sgRNAs targeting *Prdx4* exons 1–7 (E1-E7) were designed with the CRISPR design tool (http://crispr.mit.edu): sgRNA1 (forward:5'-AGCCAGCTAAAACGGCGCGCTGG-3′, reverse: 5'-CCTTGATCAGTAAATATCTTTGG-3′) and sgRNA2 (forward: 5'-GGGGCGGAGCAAGTCTCGCGAGG-3′, reverse: 5'-CACAATGACCTTTATTGAAGG-3′). *Prdx4*-positive heterozygous mice (F1 generation) were obtained by mating F0 mice with *WT* C57BL/6 J mice, and neonates were genotyped by tail PCR and sequencing.

2.3. Cell culture

KGN cells were acquired from the American Type Culture Collection (ATCC) and cultured in DMEM/F12 (Gibco, USA) supplemented with 10 % fetal bovine serum (FBS, Invitrogen, USA) and 1 % antibiotics (100 U/mL penicillin and 100 μg/mL streptomycin; Hyclone). The cells were cultured in a humidified atmosphere with 5 % CO_2 at 37 °C.

2.4. Fertility test

Female mice were paired with *WT* fertile male mice in a continuous mating scheme from 4 to 12 months of age, maintaining a ratio of female to male mice at 1:1, with a sample size of 5 per genotype. The litter counts were meticulously recorded throughout the breeding period.

2.5. Determination of oestrous cyclicity

The oestrous cycles of the mice ($n = 5$ per group) were monitored over 12 consecutive days using vaginal smears to determine their estrous cycle stages. Vaginal lavage sample were spread onto clear glass slides and stained with methylene blue. Microscopic analysis was conducted on the cell samples. We measured the duration of each cycle as the interval between two consecutive occurrences of estrus and identified the duration of each stage within the cycle. The estrous cycle was categorized into four phases: proestrus (P), estrus (E), metestrus (M), and diestrus (D).

2.6. Measurement of the estrogen levels in medium secreted from KGN

KGN cells were seeded at a density of 3×10^4 cells/well in 24-well plates. Cell growth was monitored, and transfection was initiated at approximately 50 % confluence. After reaching this point, KGN cells were treated with either *Ad-Prdx4* or *Ad-Prdx4*/siRNA virus (Vigene Bioscience, Jinan, China) and incubated for 12 h. Afterward, the medium was replaced with serum-free DMEM supplemented with Testosterone (10^{-7} M) (T1500, Sigma, USA) treated with 1 μg/mL Thapsigargin (Tg, T9033, Sigma, USA) or DMSO. The cells were then incubated for an additional 24 h. Subsequently, the culture medium was collected and stored at −20 °C for subsequent assays. Estrogen levels in the culture medium were quantified using a human enzyme-linked immunosorbent assay (ELISA) kit (CK-E10697H, FANKEL, China) following the manufacturer's instructions. For further analysis, KGN cells were reseeded in 6-well culture plates at a density of 2×10^5 cells/well, and the culture medium collected after 12 h was separately used to determine the levels of estrogen through radioimmunoassay (RIA) at the radiology department of the First Affiliated Hospital of Nanjing Medical University.

2.7. RNA isolation, reverse transcription, and RT-qPCR

Total cellular RNA was isolated utilizing TRIzol reagent (T9424, Sigma, USA) in accordance with the manufacturer's instructions. Subsequently, an equivalent amount of RNA from each sample was subjected to reverse transcription using the PrimeScriptTM RT Master Mix kit (RR036A, Takara, Japan). The resulting cDNA was utilized in real-time quantitative PCR (RT-qPCR) employing the fluorescent dye SYBR Green II (Takara, Japan). The reaction mixture for real-time PCR included 10 μL TB Green Premix Ex Taq (Takara, Japan), 0.4 μL ROX, 0.8 μL of each primer, and 1 μL template cDNA. Sterile distilled water was added to achieve a final volume of 20 μL. The reaction conditions comprised denaturation at 95 °C for 15 s, primer annealing and elongation at 60 °C for 31 s, followed by melting curve analysis with a temperature range from 60 °C to 95 °C. Target gene expression was quantified by normalizing to GAPDH expression. All experiments were conducted in triplicate and analyzed using the $2^{-\triangle\triangle Ct}$ method. The primers are listed in Supplementary Table 1.

2.8. Western blotting

Protein extracts from cells and tissues were obtained by lysing them in RIPA buffer (P0013K, Beyotime, China) supplemented with cock tail (P1030, Beyotime, China). Protein concentrations were determined using the BCA assay (Beyotime, China). Samples were prepared by diluting them in 5 × reducing (Beyotime, China) or non-reducing (EpiZyme, China) SDS loading buffer and heating at (95 ± 5)°C for 5 min with 40 μL of each sample. The proteins were separated on 6 % - 12 % sodium dodecylsulfate polyacrylamide gels (EpiZyme, China) and then transferred onto polyvinylidene fluoride membranes. After blocking with 5 % skim milk for 2 h, the membranes were incubated overnight at 4 °C with the respective primary antibodies. The following day, the membranes were washed three times with TBST solution for 5 min each and then incubated with secondary antibodies. Protein bands were visualized using an enhanced chemiluminescence (ECL, BL532A , Biosharp, China) detection system, and quantitative analysis was performed using ImageJ software. The primary antibodies used were as follows: anti-BIP (1:1000, 48584, Signalway Antibody), anti-CHOP (1:1000, 40744, Signalway Antibody), anti-ATF4 (1:1000, 49147, Signalway Antibody), anti-OS9 (1:1000, 36669, Signalway Antibody), anti-SYVN1 (1:1000, 35945, Signalway Antibody), anti-FSHR (1:1000, 22665-1-AP, Proteintech), anti-GAPDH (1:1000, 10494-1-AP, Proteintech), anti-Vinculin (1:2000, ab129002, Abcam).

2.9. TUNEL staining

TUNEL staining was conducted utilizing a One Step TUNEL Apoptosis Assay Kit (C1086, Beyotime, China) following the manufacturer's instructions. Paraffin sections were counterstained with DAPI. TUNEL-positive cell quantification was carried out as per the methodology outlined by Yan Z et al. [30]. Briefly, to eliminate histological differences between ovarian tissues, four random fields per slide (five slides per animal, five animals per group, $n = 5$) were observed. Consequently, a total of 100 random fields ($5 \times 5 \times 4 = 100$) per group were analyzed. The number of TUNEL-positive granulosa cells and total granulosa cells within the antral follicles were counted. The percentage of TUNEL-positive granulosa cells (%) within the antral follicles was analyzed using ImageJ software.

2.10. Serum preparation and hormone assays

Blood samples were collected at various stages of the oestrous cycle. Subsequently, the samples underwent centrifugation at 3000 rpm for 15 min. The serum was harvested and stored at −80 °C. Serum oestradiol (E_2) levels were measured using a radioimmunoassay performed at the radiology department of the First Affiliated Hospital of Nanjing Medical University following the protocol provided by the manufacture.

2.11. Haematoxylin and eosin (H&E) staining and follicle counting

Ovaries ($n = 5$ per group) were fixed with 4 % paraformaldehyde overnight and subsequently prepared for histological analysis using established protocols. Tissues samples were sectioned into 4-μm-thick slices and subjected to H&E staining. Follicle counting was conducted following the procedures outlined with slight adjustments [24]. The follicle count within each category was independently performed by two researchers blinded to the group assignments.

2.12. Transmission electron microscopy

KGN cells subjected to various treatments (outlined below) were harvested by scraping and centrifugation. Both KGN cells and ovaries were then fixed in 2.5 % glutaraldehyde and embedded in 4 % agarose. The samples underwent postfixation in 1 % osmium tetroxide dissolved in phosphate buffer for 1 h, followed by triple washing and dehydration in an ethanol gradient (25, 50, 75 and 96 % for 2 rounds of 10 min each, and 100 % for 2 rounds of 15 min each). Subsequently, the slices were placed in 100 % acetone for 2 rounds of 20 min each, followed by immersion in a mixture of acetone and Epon resin poly/bed-812 (1:1) overnight. Afterward, the specimens were placed onto pure resin for at least 4 h before embedment in new pure resin and polymerization at 60 °C for 48 h. The specimen, embedded in resin, was cut into 50 nm sections using a Powertome and placesd on copper grids coated with a thin film of pioloform. Subsequently, the grids were stained with 4 % uranyl acetate for 30 min at 40 °C and 0.5 % lead citrate for 2 min at room temperature. The sections were then examined using a JEM-1400 Flash electron microscope. Analysis was conducted on sections from both control and cut-treated slices, with a total of 3 slices in each group.

2.13. Statistical analysis

All data were analyzed using GraphPad Prism 8.0 (GraphPad Software, San Diego, CA) and presented as means ±SEM. Group comparisons were analyzed by the Student's *t*-test or One-way analysis of variance (ANOVA). The *t*-test was utilized for comparing two groups, whereas One-way ANOVA was employed for comparisons involving three or more groups. In addition, variations in study outcomes related to age and genotype were assessed using a two-way ANOVA test, with consideration given to the interaction term. Statistical significance was defined as $P < 0.05$. The sample sizes ("*n*"), statistical tests and corresponding *P* values were detailed in each figure legend.

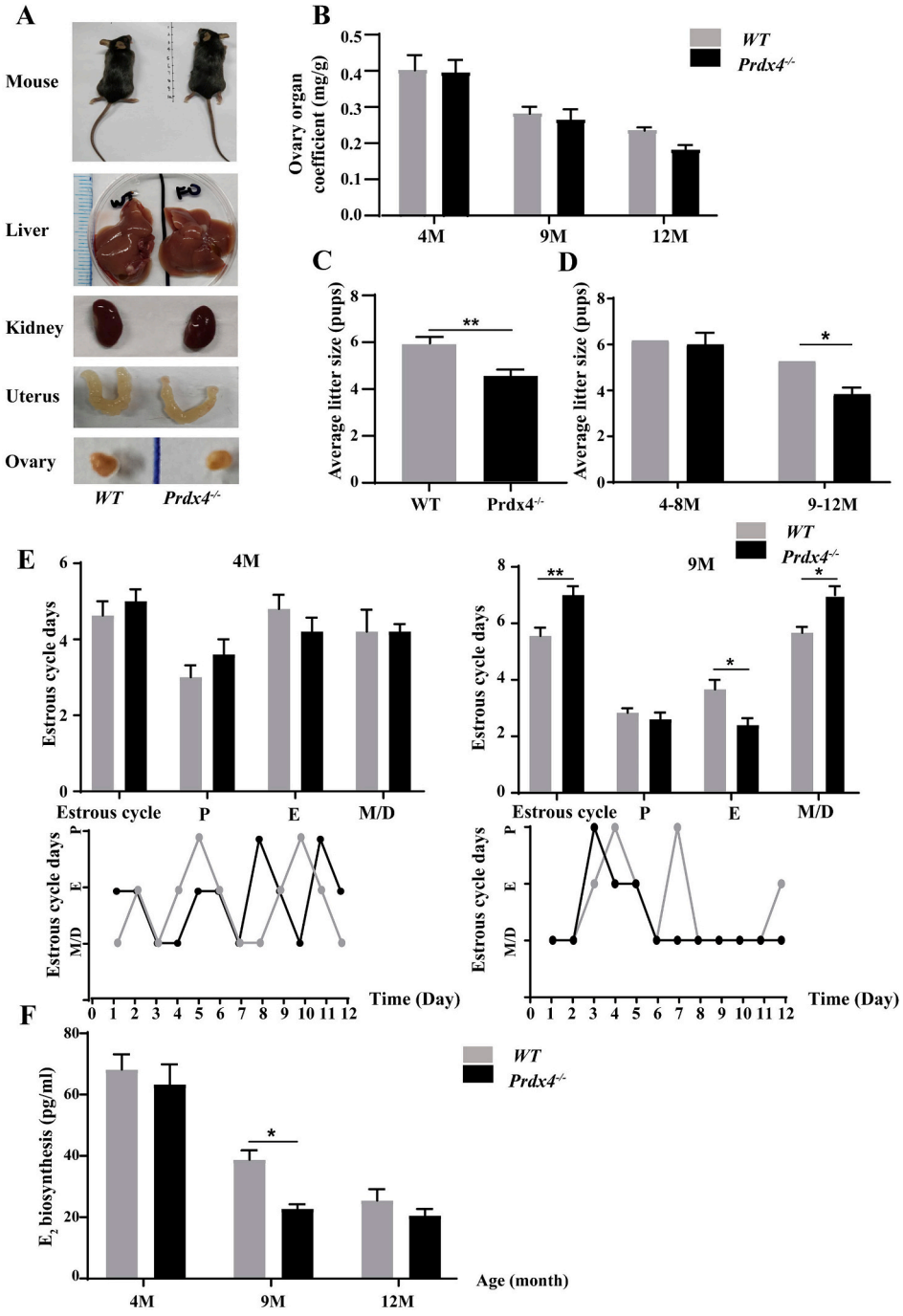

Fig. 1. *Prdx4* knockout aggravated reproductive aging. A Representative photographs showing the appearance and some vital organs from *WT* mice and *Prdx4*$^{-/-}$ mice. There were no difference between *Prdx4*$^{-/-}$ and *WT* mice at all ages. $n = 5$ per group. B Ovary organ coefficient of *WT* and *Prdx4*$^{-/-}$ mice at different ages. $n = 5$ per group. Data are shown as means ± SEM. Statistical analyses were performed by two-way ANOVA. C Average litter size of *WT* and *Prdx4*$^{-/-}$ mice were analyzed. Data are shown as means ± SEM. $n = 5$ per group. Statistical analyses were performed by Student's *t*-test. D Mean litter size of *WT* and *Prdx4*$^{-/-}$ mice at various ages were compared. $n = 5$ per group. Data are shown as means ± SEM. Statistical analyses were performed by two-way ANOVA test. E The average lengths of the estrous cycle and the duration of proestrus (P), estrus (E), metestrus (M), and diestrus (D) were assessed using vaginal cytology over a 12-day period in mice aged 4 and 9 months. $n = 5$ per group. Statistical analyses were performed by Student's *t*-test. F Serum E_2 levels during dioestrus were measured in *Prdx4*$^{-/-}$ and *WT* mice at all ages. $n = 5$ per group. Data are shown as means ± SEM from three independent experiments. Statistical analyses were performed by two-way ANOVA.*P value <0.05, **P value <0.01.

3. Results

3.1. Prdx4 knockout aggravated reproductive aging

To evaluate the effect of PRDX4 on female fertility during aging, we established *Prdx4*$^{-/-}$ mouse model and identified the genotypes following our previous study [15]. We compared development, growth, and reproduction of *Prdx4*$^{-/-}$ and *WT* littermates. *Prdx4*$^{-/-}$ mice were normal in development and growth. The gross morphology of liver, kidney, uterus and ovarian organic coefficient did not differ between *Prdx4*$^{-/-}$ and *WT* mice at all ages (Fig. 1A, B). The results of two-way ANOVA revealed a significant interaction between two factors, age and type on ovarian organ coefficient ($F(2,24) = 6.911$, $P = 0.0043$, the proportion of the total variation $\eta^2 = 4.715$ %). This finding suggests that the protective effect of PRDX4 on ovarian function becomes more prominent with advancing age. Notably, a totally significant reduction of the average litter size was observed in *Prdx4*$^{-/-}$ mice during aging (after 9 months old) but was at the same level in 4-month-old *Prdx4*$^{-/-}$ mice as *WT* mice at the same age ($P < 0.05$, Fig. 1C, D). A more severe disruption of the hypothalamic-pituitary-ovary (HPO) axis was observed in *Prdx4*$^{-/-}$ mice. Daily vaginal smears were used to determine the estrous cycle. As shown by the results, the *WT* group had regular estrous cycles with a duration of 4–5 days. However, the *Prdx4*$^{-/-}$ group showed irregular estrous cycles with a decrease in oestrus period and an increase in dioestrus period during aging (9 months old) (Fig. 1E). We then collected sera and measured the levels of E_2. E_2 levels showed a significant decrease in aging (9 months old) *Prdx4*$^{-/-}$ mice compared to *WT* mice ($P < 0.05$, Fig. 1F).

3.2. Age-related changes in the ovaries were accelerated due to PRDX4 deficiency

In order to investigate whether age-related decline of ovarian reserve is accelerated due to PRDX4 deficiency, we compared follicle numbers of every grade in ovaries at 4 and 9 months old between *WT* and *Prdx4*$^{-/-}$ mice. The data suggested that ovaries from *Prdx4*$^{-/-}$ mice at 9 months old retained a poorer pool of follicles than *WT* group. However, there was no significant difference at 4 months old. To be specific, less

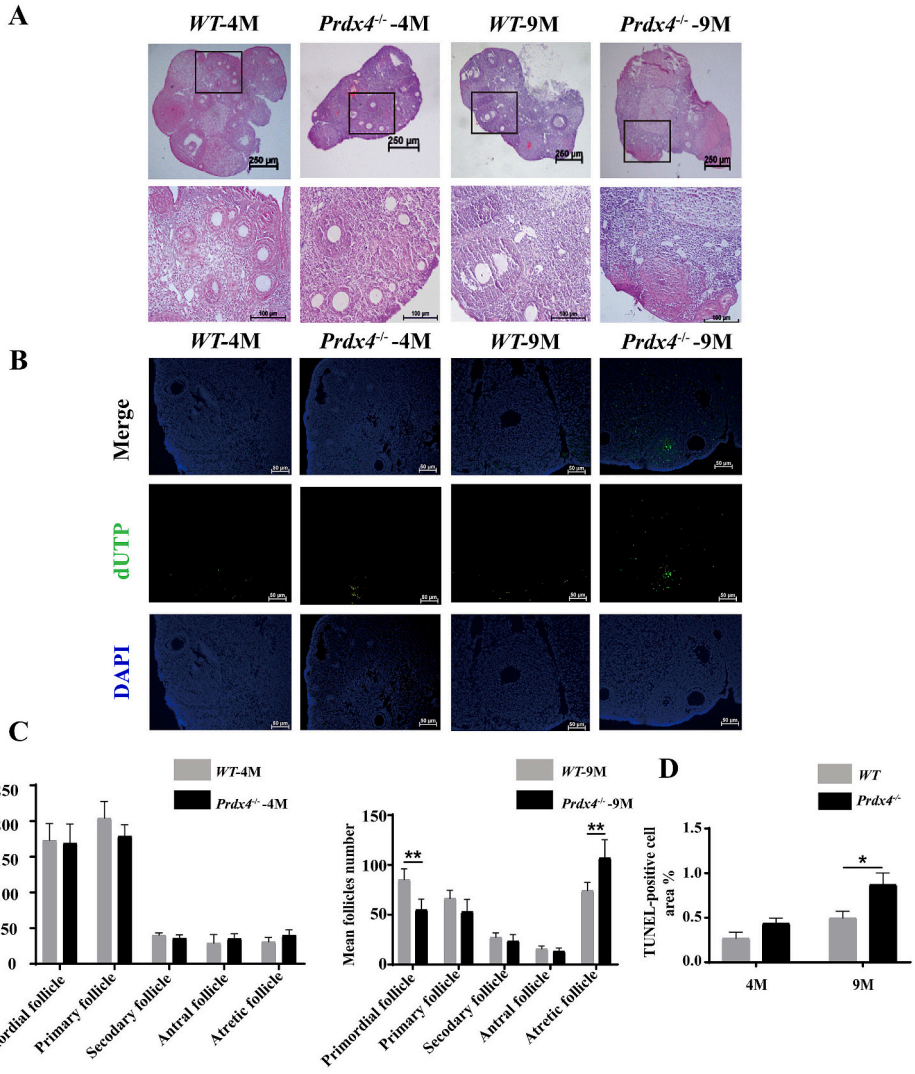

Fig. 2. Age-related changes in the ovaries were accelerated due to PRDX4 deficiency. A Histology of ovarian sections from *Prdx4*$^{-/-}$ and *WT* groups at different ages. $n = 5$ per group. Scale bar = 250 μm at × 4 magnification; scale bar =100 μm at × 20 magnification. B Ovaries obtained from *Prdx4*$^{-/-}$ and *WT* mice aged 4 and 9 months were utilized to detect apoptosis via an in situ TUNEL fluorescence assay (×20). In this assay, the nuclei of TUNEL-positive (apoptotic) cells were labeld green. Scale bar =50 μm. $n = 5$ per group. C The summary of follicle counts at various developmental stages in *Prdx4*$^{-/-}$ and *WT* mice aged 4 and 9 months is provided. $n = 5$ per group. All data are shown as means ± SEM. Statistical analyses were performed by Student's *t*-test. D A comparison was made regarding the number of TUNEL-positive granulosa cells between *Prdx4*$^{-/-}$ and *WT* mice aged 4 and 9 months. $n = 5$ per group. All data are shown as means ±SEM. Statistical analyses were performed by two-way ANOVA. *P value <0.05, **P value <0.01.

primordial follicle and more atretic follicles were observed in *Prdx4*$^{-/-}$ mice comparable to those in *WT* mice at 9 months old ($P < 0.01$, Fig. 2A, C). Since follicle atresia is associated with granulosa cell apoptosis [18], we compared granulosa cells apoptosis among each group. The result showed that more apoptotic cells were detected in ovaries from the 9-month-old *Prdx4*$^{-/-}$ mice compared to ovaries from *WT* mice, although there were no significant changes between two groups in the 4-month-old ($P < 0.05$, Fig. 2B, D). These findings revealed the crucial role of PRDX4 in delaying ovarian aging.

3.3. ER homeostasis was significantly altered in granulosa cells of aging *Prdx4*$^{-/-}$ mice

ER stress is the closely linked event in cell homeostasis and apoptosis [15]. The expanded ER, the increased numbers of lipid droplets and residual bodies reveal the ongoing degeneration of ER homeostasis. So ultrastructural changes in granulosa cells of each group were evaluated by electron microscopy. As compared to *WT* mice, the granulosa cells of 9-month-old *Prdx4*$^{-/-}$ mice had significantly increased dilated ER cisternae, lipid levels and residual bodies (Fig. 3A). As the enlarged

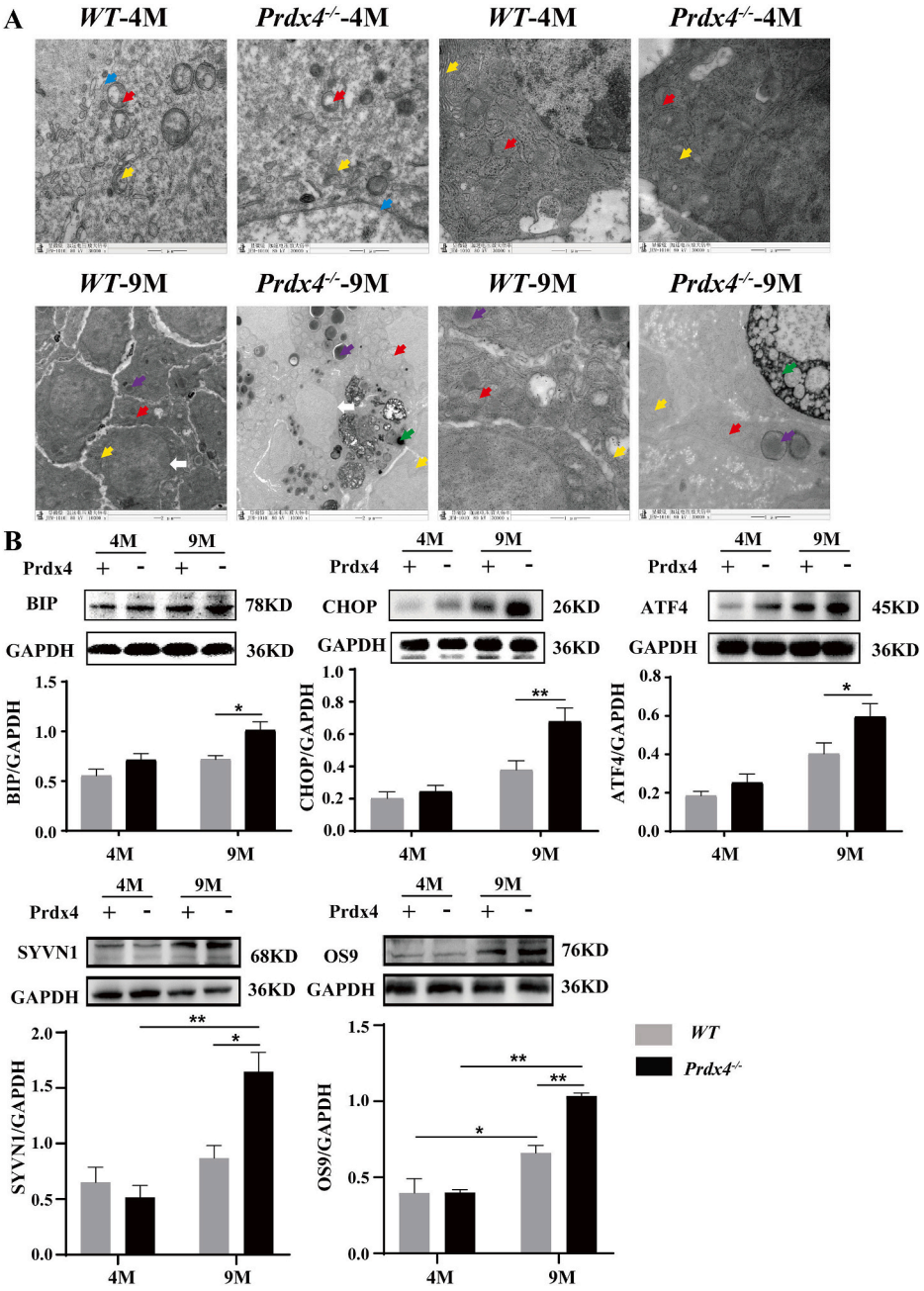

Fig. 3. ER homeostasis was significantly altered in granulosa cells of aging *Prdx4*$^{-/-}$ mice. A Representative electron micrographs of 4- and 9-month-old *WT* and *Prdx4*$^{-/-}$ granulosa cells [zona pellucida (blue arrow), mitochondria (red arrow), endoplasmic reticulum (yellow arrow), nucleus (white arrow), residual corpuscles (green arrow), lipid droplets (purple arrow)]. Scale Bars: 1 μm, 2 μm. $n = 5$ per group. B Western blot analysis with representative ER stress and ERAD pathway-associated factors including BIP, CHOP, ATF4, SYVN1 and OS9 levels in the ovary of 4- and 9-month-old *WT* and *Prdx4*$^{-/-}$ mice. Densitometric analysis is shown as means ± SEM, $n = 3$ independent experiments. Statistical analyses were performed by *t*-test and two-way ANOVA.*P value <0.05, **P value <0.01.

endoplasmic reticulum (ER) is a distinctive feature of the unfolded protein response (UPR) to ER stress, we conducted immunoblot analyses to investigate ER stress markers. As shown in Fig. 3B, the expression level of ER stress marker - BIP and ATF4 was relatively increased in 9-month-old *Prdx4*$^{-/-}$ female mice ($P < 0.05$). The expression of CHOP, which mainly activated the cell death pathway triggered by ER stress, was also significantly increased in the 9-month-old *Prdx4*$^{-/-}$ female mice compared to *WT* mice ($P < 0.01$). The results of two-way ANOVA indicated a significant interaction between age and genotype on CHOP protein expression ($F(1,12) = 5.074$, $P = 0.044$, $\eta^2 = 9.317$ %), indicating elevated aging-related endoplasmic reticulum stress and accelerated apoptosis of granulosa cells in the ovaries due to PRDX4 deficiency. The process of endoplasmic reticulum-associated degradation (ERAD) is accountable for eliminating misfolded proteins within the ER through cytosolic proteasomal degradation [31]. We then further examined the expression of the ERAD marker genes OS9 and SYVN1 (Fig. 3B). The expression levels of SYVN1 and OS9 significantly elevated in the 9-month-old *Prdx4*$^{-/-}$ group compared to *WT* mice ($P < 0.05$ and $P < 0.01$). Notably, our analyses revealed strong significant interactions between age and genotype on OS9($F(1,8) = 35.33$, $P < 0.001$, $\eta^2 = 12.62$ %) and SYVN1 protein expression ($F(1,18) = 17.24$, $P < 0.001$, $\eta^2 = 25.26$ %), implying accelerated ERAD activation with the aging process as a result of the lack of PRDX4. The activated ER stress and ERAD pathway further described the significantly altered ER homeostasis in

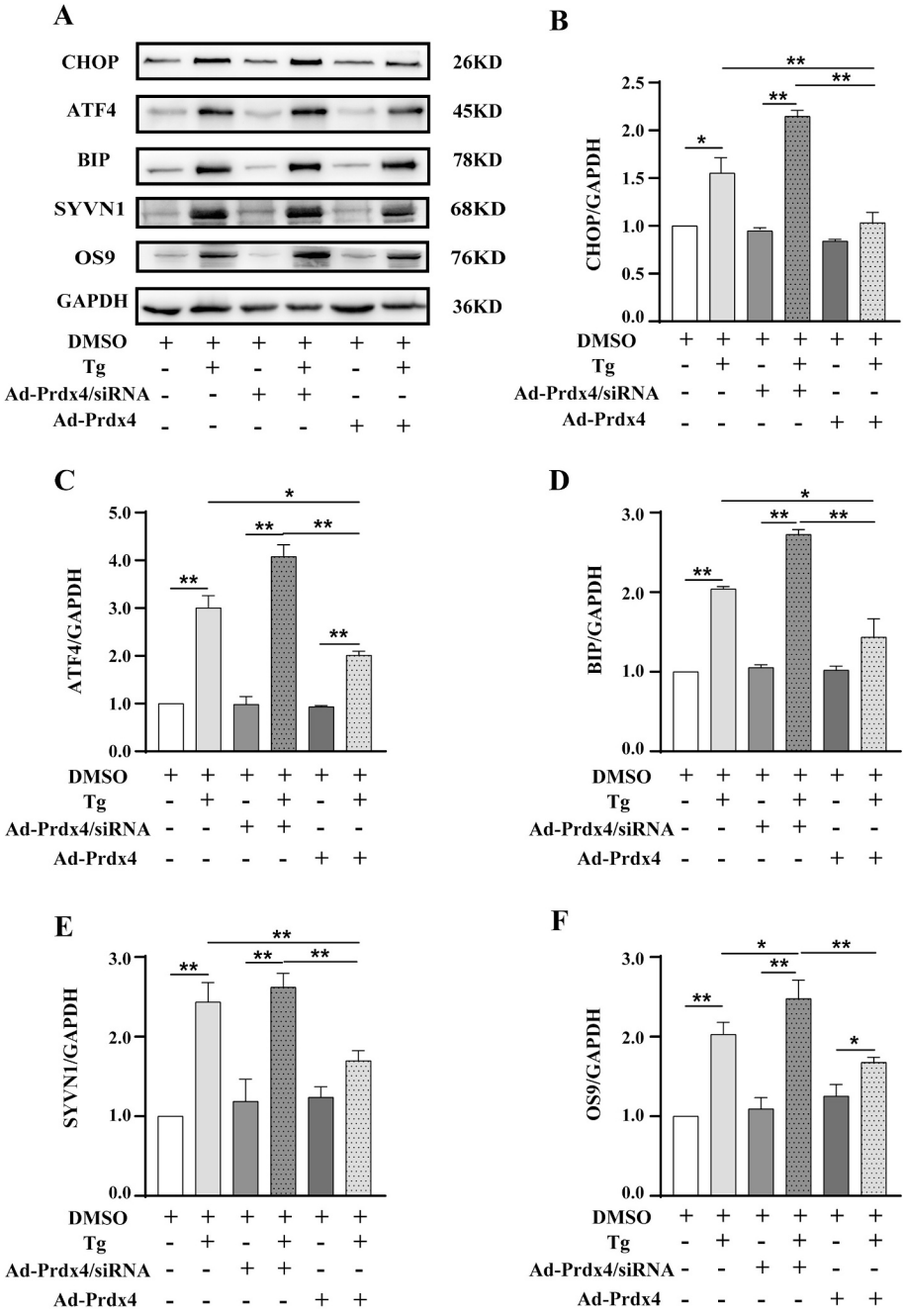

Fig. 4. Overexpression of *Prdx4* restored ER homeostasis in the Tg-treated KGN cells. A *Prdx4* knockdown and overexpression KGN cells were established and treated with DMSO or combined with Tg. Western blot analysis for representative ER stress and ERAD pathway-associated factors including CHOP, ATF4, BIP, SYVN1 and OS9 levels in KGN cells were compared among different treatment groups. B-F The CHOP, ATF4, BIP, SYVN1 and OS9 protein expression levels were quantitatively analyzed. Densitometric analysis is shown as means ± SEM, $n = 3$ independent experiments. Statistical analyses were performed by one-way ANOVA. *P value <0.05, **P value <0.01.

granulosa cells due to PRDX4 deficiency during aging. Although there are minimal biological differences among individual mice, the current study has limitations in terms of sample size and the generalizability of the findings. Future research should aim to replicate these findings with larger and more diverse samples to confirm the robustness of the interaction effect.

3.4. Overexpression of Prdx4 restored ER homeostasis in the Thapsigargin-treated KGN cells

To further investigate the mechanism underlying the role of PRDX4 on maintaining protein homeostasis in granulosa cells, we constructed *Prdx4* knockdown and overexpression KGN cell lines by adenoviral vector as described in our previous study [32]. Thapsigargin (Tg) is one of the most popular inducers of sustained ER stress [33] and then simulate aging process in granulosa cells. We found the optimal Tg concentration with ER stress is 1 μg/mL by PCR (Supplement Fig. 1). So we used 1 μg/mL Tg to induce ER stress in KGN cells and incubated an equal dose of DMSO as a control. We treated control group, knockdown group, overexpression group with DMSO or combined with Tg respectively. We then examined the expression of ER stress marker proteins and the ERAD marker proteins upon *Prdx4* knockdown and overexpression KGN cells.

As exhibited in Fig. 4A, the addition of Tg induced ER stress as evidenced by an increase in the expression level of the ER stress marker, ATF4, BIP and CHOP in all groups ($P < 0.05$, $P < 0.01$ and $P < 0.01$). And the levels of ERAD related proteins OS9 and SYVN1 were also much higher in Tg-treated group than in DMSO-treated group (both $P < 0.01$). Moreover, ER stress level and ERAD activities were prominently higher in the PRDX4 deficiency group as *Ad-Prdx4*/siRNA markedly increased the levels of ATF4, BIP, CHOP, OS9 and SYVN1, while the addition of *Ad-Prdx4* significantly reversed this effect (Fig. 4B-F). These results verified the effect of PRDX4 on restoring ER homeostasis in granulosa cells during aging process.

3.5. PRDX4 deficiency impacted FSHR synthesis and reduced oestradiol secretion

To determine whether *Prdx4* overexpression improves estrogen (E_2) biosynthesis in KGN cells, we measured the levels of E_2 by using testosterone as a substrate. We observed that in KGN cell when treated with Tg, *Prdx4* overexpression resulted in increased levels of E_2 levels compared with the control group ($P < 0.05$) and knockdown group ($P < 0.01$) while no significant difference among other three groups treated without Tg (Fig. 5A). Then we examined the level of FSHR in mice ovaries using western blot. Significantly decreased FSHR expression was detected in the 9-month-old *Prdx4*$^{-/-}$ mouse group compared with *WT* mice at the same age ($P < 0.01$, Fig. 5B). Similarly, we also found that the knockdown group showed decreased levels of FSHR compared with control group when treated with Tg ($P < 0.01$) and back to normal levels in overexpression group whereas FSHR protein levels didn't differ among other groups treated without Tg (Fig. 5C). These results revealed that PRDX4 deficiency dramatically affects FSHR synthesis and reduces oestradiol secretion during aging. Overexpression of *Prdx4* in KGN cells were correlated with a significant rescue of the senescence phenotype.

3.6. PRDX4 deficiency compromised the expression of FSHR especially the functional trimer, which can be rescued by Prdx4 overexpression

FSHR, existing as a functional trimer [27], is rich in disulfide bonds [26], and its mysterious hinge region consists of two unique sequence motifs coupled by three disulfide bonds, ensuring the structural integrity and stability of the FSHR configuration [28,29]. It is one of the major genes that protecting the ovary function and is highly expressed in granular cells. So, we investigated whether the deficiency of PRDX4 compromised the normal conformation of FSHR and then exacerbated the progression of ovarian aging in aging *Prdx4*$^{-/-}$ mice. As shown in Fig. 6A, there was no obvious abnormality in the ER structure of KGN cells treated with DMSO. The ER of KGN cells treated with 1 μg/mL Tg to simulate the cell senescence model was dilated compared with the control group treated with DMSO. Tg induced more obvious ER swelling, expansion, and proliferation in *Prdx4* knockdown groups, while *Prdx4* overexpression reduced ER expansion and back to normal (Fig. 6A). Nonreducing western blot was used to detect the functional trimer of FSHR in two groups of mice ovaries. Our study showed that the functional trimer of FSHR was significantly decreased while the monomer and dimer increased in ovaries from 9-month-old mice than 4-month-old mice both in *WT* group and *Prdx4*$^{-/-}$ group ($P < 0.05$). During ovarian hypofunction (9 M), the monomer and dimer of FSHR were significantly increased while the functional trimer of FSHR was significantly decreased in ovaries from *Prdx4*$^{-/-}$ mice than *WT* mice ($P < 0.05$) (Fig. 6B). In KGN cell lines, the monomer and dimer had no changes both in *Prdx4* overexpression group and knockdown group with DMSO treatment only. After being treated with 1 μg/mL Tg, the monomer and dimer were significantly increased compared with DMSO treatment ($P < 0.01$). In *Prdx4* knockdown group, Tg could induce

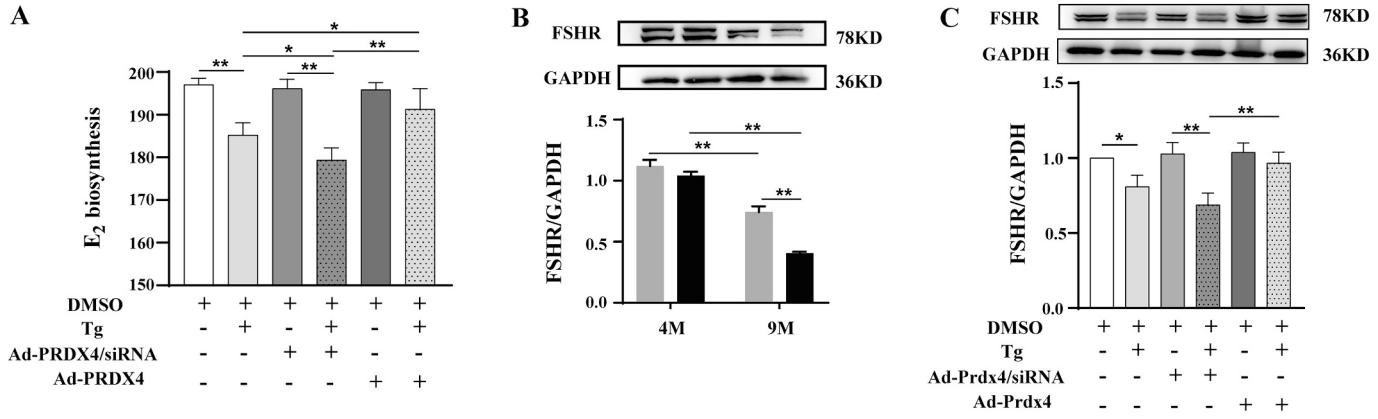

Fig. 5. PRDX4 deficiency affected FSHR synthesis and reduced oestradiol secretion. A Mean E_2 levels secreted from *Prdx4* knockdown and overexpression KGN cells treated with DMSO or combined with Tg were evaluated by ELISA. $n = 3$ independent experiments. Densitometric analysis is shown as means ± SEM. Statistical analyses were performed by one-way ANOVA. B Western blot for FSHR levels was analyzed in the ovary of 4- and 9-month-old *WT* and *Prdx4*$^{-/-}$ mice. $n = 3$ independent experiments. Densitometric analysis is shown as means ± SEM. Statistical analyses were performed by two-way ANOVA. C The levels of FSHR in KGN cells from *Prdx4* knockdown and overexpression KGN cells treated with DMSO or combined with Tg were evaluated using western blot. Densitometric analysis is shown as means ± SEM, $n = 3$ independent experiments. Statistical analyses were performed by one-way ANOVA. *P value <0.05, **P value <0.01.

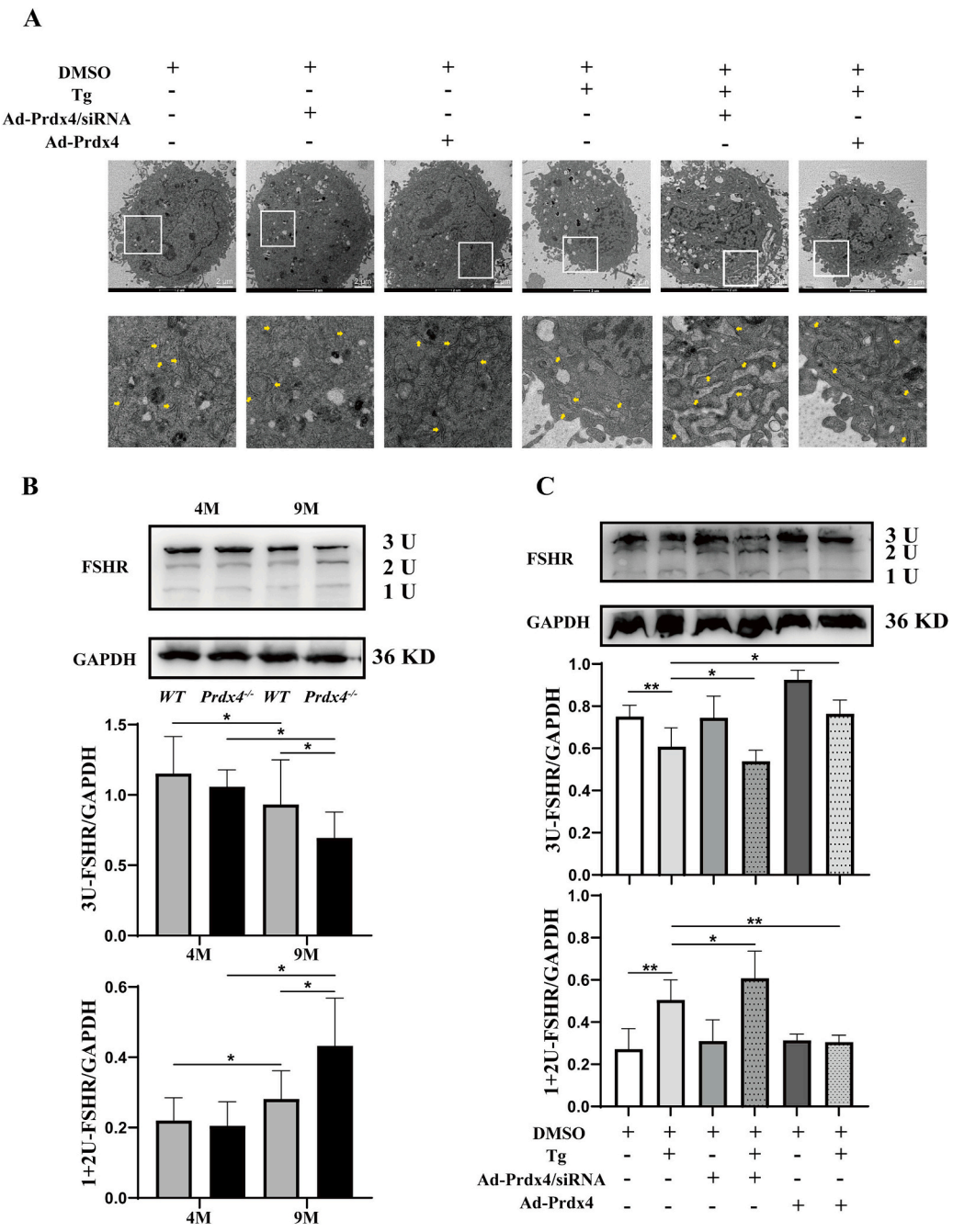

Fig. 6. PRDX4 deficiency compromised the oxidative folding of FSHR which can be rescued by *Prdx4* overexpression. A Representative electron micrographs of KGN cells from *Prdx4* knockdown and overexpression KGN cells treated with DMSO or combined with Tg. ER dilation is the most important morphological feature in Tg treatment group, especially in the *Prdx4* knockdown KGN cells treated with Tg [endoplasmic reticulum (yellow arrow)]. Scaler Bars = 2 μm. B Monomer, dimer and functional trimer of FSHR were detected by Non-Reducing Western Blot in the ovaries of 4-and 9-month-old *WT* and *Prdx4*$^{-/-}$ mice. $n = 3$ independent experiments. Densitometric analysis was shown as means ± SEM. Statistical analyses were performed by two-way ANOVA. C Monomer, dimer and functional trimer of FSHR were detected by Non-Reducing Western Blot in the KGN cells from *Prdx4* knockdown and overexpression KGN cells treated with DMSO or Tg. $n = 3$ independent experiments. Densitometric analysis is shown as means ± SEM. Statistical analyses were performed by one-way ANOVA. **P* value <0.05, ***P* value <0.01.

dramatically increased FSHR monomer and dimer and decreased trimer compared with Tg treatment only ($P < 0.05$), but reverted to normal in Tg treatment group with *Prdx4* overexpression (Fig. 6C). The results of this study suggest that the deficiency of PRDX4 has a substantial impact on the expression of FSHR, especially the functional trimer, due to impaired disulfide bond formation. Overexpression of *Prdx4* in KGN cells correlated with a significant rescue of this phenotype.

4. Discussion

Ovarian aging occurs much faster than somatic aging in human, so exhibits prolonged post-reproductive lifespans. The mechanisms underlying this phenomenon have proved to be challenging to determine. Granulosa cells are one of the main ovarian cell types, which mainly act on steroidogenesis and folliculogenesis regulation. It has long been considered that the impaired function of granulosa cell is closely related to ovarian aging [7,36], but the underlined mechanisms are still limited.

The aging process contains a number of features, which suggests that ER stress is activated, such as the accumulation of harmful protein modifications, protein misfolding and aggregation, and the impairment of global protein synthesis [37]. Loss of cellular proteostasis, recently defined as one of the major causes of aging [12], has rarely been investigated in the context of the ovarian aging. PRDX4 is involved in enhancing the efficiency of oxidative protein folding in ER, and then plays a critical role in maintaining protein homeostasis [13]. As revealed in our previous study, PRDX4 was expressed at a high expression level in granulosa cells and protected the ovary from oxidative damage [38,39]. It helped to prevent ovarian granulosa cell apoptosis through inhibiting oxidative stress and ER stress-related pathways [15]. In this study, we identified that PRDX4 is a crucial factor that contributes to delaying ovarian aging during the natural aging process. Regarding the mechanism, PRDX4 is fundamental for protein homeostasis maintenance in granulosa cells. PRDX4 deficiency contributes to granulosa cells apoptosis by destroying ER protein homeostasis, and then triggering ER stress. The particularly important is that PRDX4 deficiency leads to markedly reduced expression of FSHR, especially the functional trimer, due to impaired disulfide bond formation. And the unusual conformation of FSHR severely damages FSHR function, resulting in decrease of E_2 levels and imbalance of granulosa cell protein homeostasis, further aggravating ovarian aging.

In this study, we observed the fertility-related changes of *Prdx4*$^{-/-}$ female mice during natural aging and found that PRDX4 is an important protective factor for delaying ovarian aging. Mice are considered sexually mature at the age of 3 to 6 months, and the endocrine equivalent of human perimenopause is 8 to 9 months [40]. *Prdx4*$^{-/-}$ mouse only shows minor phenotypic abnormalities as described in previous studies [35]. However, compared to age-matched wild-type controls, the significantly reduced average liter size, disordered estrous cycles, decreased E_2 level, and high atresia follicle proportion of the *Prdx4*$^{-/-}$ mouse group during aging supported an aggravated decline in ovarian function. As the central importance of follicles to maintaining female reproductive and endocrine function, ovarian life span is determined by the number of follicles present in the ovary [2]. High atresia follicle proportion is one of the important hallmarks of ovarian aging. Granulosa cells play an essential role in follicle development because they provide nutrients and mechanical support for oocytes via physical interactions [8]. Our data revealed the significantly increased apoptosis of ovarian granulosa cells in 9-month-old *Prdx4*$^{-/-}$ mice, which accounted for the accelerated ovarian aging. These observations were consistent with other studies, which also indicated that *Prdx4* knockdown exacerbated apoptosis [41,42]. Moreover, a preliminary analysis of cynomolgus monkeys ovary by single-cell transcriptome sequencing technology identified that PRDX4 is a new molecular marker of granulosa cell aging [16], which further verified our conclusion.

Our observations suggested that the aggravated ER dyshomeostasis of *Prdx4*$^{-/-}$ mice ovary was more severely during natural aging. Due to the lack of PRDX4, it challenged the protein folding environment in the ER of ovarian granulosa cells. ER is responsible for the production and folding of secreted proteins. The accumulation of misfolded proteins in the ER triggered UPR by activating three main UPR sensors, including IRE1α, PERK and ATF6 on the ER membrane [24]. UPR is activated in response to the accumulation of misfolded proteins, while ERAD is responsible for clearing away misfolded proteins in the ER for cytosolic proteasomal degradation [31]. When UPR cannot restore correct protein folding, ER stress ensues. Severe and persistent ER stress plays a crucial role in granulosa cell apoptosis [43]. During the aging process, a gradual accumulation of intracellular aggregates composed of misfolded proteins occurs within organisms, which is accompanied by a significant decline in the compensatory capacity of the proteostasis network and a consequent decrease in tissue and cellular compensatory function [44]. Ovary undergoes highly dynamic cellular molecular and genetic changes, such as follicular development and oocyte growth controlled by growth factors and cytokine. These reproductive changes challenge ER to compensate for the extensive protein secretion. Based on this hypothesis, it is likely that deficiency of PRDX4, which is involved in enhancing the efficiency of oxidative protein folding, decreases ovarian compensatory function and increases age-related ER stress in aging ovary. Our data revealed that PRDX4 deficiency triggered ER stress and elevated the ERAD pathway, which suggested that increased ER dyshomeostasis in ovary was more severely due to PRDX4 deficiency during aging. In 9-month-old *Prdx4*$^{-/-}$ mice, the ER of granulosa cells expanded, and the number of lipid droplets and residual bodies increased, suggesting the ongoing degeneration of ER homeostasis. We found that knockout of *Prdx4* had no influence on phenotype compared with *WT* mice at the age of 4 months, which verified redundant mechanisms of oxidative protein folding in mammalian cells [45]. However, this redundant mechanism is not sufficiently basic for this role during aging. Correspondingly, the conspicuous induction of ER dyshomeostasis was observed after *Prdx4* knockdown in the KGN cell line when treated with Tg and could be rescued by overexpression of *Prdx4*. These findings are consistent with previous reports that elevated ER stress was observed under particular pathological condition, such as DSS or D-gal induced oxidative damage in *Prdx4*-knockout mice [15,46]. Our data revealed that due to PRDX4 deficiency aggravated ER dyshomeostasis results in increased apoptosis of ovarian granulosa cells and then impairs the function of granulosa cell, which is closely related to accelerated ovarian aging [7,36].

In this study, we also found that PRDX4 deficiency led to markedly reduced expression of FSHR, especially the functional trimer. The *Fshr* gene has been identified as the first gene causing nonsyndromic primary ovarian insufficiency (POI) [47]. FSHR, which is mainly expressed in granulosa cells [48], has been suggested as one of the etiological factors in the development of POI [25]. It involves in normal reproductive function, which can regulate the development and maturation of oocytes and follicles, and stimulate estrogen and progesterone production by granulosa and thecal cells [25]. The fact that FSHR is rich in disulfide bonds [26] and its mysterious hinge region consists of two unique sequence motifs coupled by three disulfide bonds which ensure an integrated and stable conformation of the FSHR structure [28,29] leads us to investigate whether PRDX4 deficiency would induce unusual conformation of FSHR and then contributes to ovarian aging. Here, we observed less functional trimer of FSHR in the ovary of 9-month-old *Prdx4*$^{-/-}$ mice. The unusual conformation of FSHR affect its function, resulting in decrease of E_2 levels and imbalance of granulosa cell protein homeostasis, further aggravating ovarian aging. Our findings are consistent with previous findings in which patients with a partial loss-of-function mutations of FSHR displayed a mild phenotype with POI [49].

Furthermore, the differences between knockdown and overexpression of *Prdx4* in KGN cell under ER stress conditions highlighted the special role of PRDX4 in disulfide bond formation and protein homeostasis maintenance during cellular senescence. When treated with DMSO, their phenotype showed no difference compared with control group, which was consistent with the results of young mice. When treated with Tg, knockdown of *Prdx4* in KGN cells showed the same phenotype with aging mice. Tg, a specific irreversible inhibitor of ER Ca^{2+}-ATPase, can induce sustained ER stress [33] and then simulate aging process in granulosa cells. When treated with Tg, overexpression of *Prdx4* increased the expression of FSHR, especially the functional trimer, maintained ER proteostasis in granulosa cell, and enhanced E_2 levels. These findings strongly pointed out that PRDX4 enhances the ability of senescent granulosa cell to promote protein folding properly, which can maintain ER proteostasis and delay ovarian aging. The data from our study revealed one of the major molecular mechanism of ovarian aging, in which impaired misfolded proteins consequent to PRDX4 deficiency triggers ER stress, contributing to proteostasis failure and ultimately leading to the apoptosis of ovarian granulosa cells.

In summary, our study emphasizes the critical role of granulosa cell endoplasmic reticulum proteostasis in ovarian aging, identifying PRDX4 as a key protein for the buffering capacity of the proteostasis network.

Considering the significance of proteostasis collapse on aging from nematodes to humans [12,50,51], and the conclusions drawn from our prior research connecting PRDX4 to human ovarian aging, PRDX4 could potentially serve as a significant target for postponing the process of human ovarian aging. Therefore, it is imperative to conduct further in-depth research to validate these findings in human and thoroughly investigate the underlying mechanisms. In the future, increased focus should be placed on investigating the restorative impacts of elevated PRDX4 expression in aged human ovarian granulosa cells, with the aim of restoring protein homeostasis and improving oocyte quality. These studies will also contribute to develop potential treatment strategies for PRDX4 deficiency, such as under the natural process of ovarian aging. Currently , multiple studies have demonstrated the potential of novel small molecules to selectively target UPR components and regulate endoplasmic reticulum protein homeostasis, offering new avenues for intervening in aging [52–55]. However, it is crucial to consider the potential side effects of UPR-targeting medications, such as liver failure, impaired immune system function, pancreatic issues, and other disorders [56]. Therefore, gene therapy for PRDX4 deficiency or screening of small-molecule compounds targeting PRDX4-related pathway may hold promise as a potential therapeutic strategy to locally restore ER protein homeostasis, increase FSHR expression in granulosa cells, and consequently restore ovarian function.

5. Conclusion

This study presents the initial analysis of PRDX4's role in facilitating the functional spatial conformation of the crucial protein FSHR, thereby mitigating ovarian aging during the corresponding perimenopause phase in female mice. We acknowledged the limitations of using KGN cells to investigate the underlying mechanism. KGN maintains most physiological activities, including the expression of functional FSHR, as well as the same pattern of steroidogenesis observed in normal granulosa cells, which allows us to study various aspects of physiological regulation [34]. On the other hand, we have studied the effect of PRDX4 deficiency where we cannot separate the local from the systemic effects, although *Prdx4*$^{-/-}$ mouse only shows minor phenotypic abnormalities as described in present and previous studies [35]. Thus, the focus of future investigations should be on ovarian-specific, ovarian-restricted manipulation.

In conclusion, PRDX4 is a necessity for maintaining protein homeostasis in granulosa cells. The deficiency of PRDX4 would trigger accelerated ovarian aging due to exacerbated ER stress, and finally increasing granulosa cells apoptosis. The most intriguing is that PRDX4 improves the expression of FSHR, especially the functional trimer, and reduces ER stress in granulosa cells, thereby enhancing hormonal and fertility related characteristics. Based on the decreased expression of PRDX4 in human ovary during normal aging as we observed in previous study, PRDX4 provides a promising therapeutic target in maintaining female fertility and improving the pregnant outcome of patients with diminished ovarian reserve from the perspective of ER protein homeostasis.

Abbreviations

PRDX4	Peroxiredoxin 4
FSHR	Follicle-stimulating hormone receptor
PDI	protein disulfide isomerase
ERO1	ER oxidoreductase 1
ERAD	Endoplasmic reticulum associated degradation
POI	primary ovarian insufficiency

Ethics approval and consent to participate

All animals care and experimental procedures were conducted in accordance with the Institutional Guidelines of the Animal Care and Use Committee (IACUC) and were approved by the IACUC of Nanjing Medical University (IACUC - 1,711,029).

Consent for publication

Not applicable.

Funding

This work was supported by the National Natural Science Foundation of China (82271668) and Open Funding of State Key Laboratory of Reproductive Medicine and offspring health (SKLRM-K202203).

CRediT authorship contribution statement

Xiaofei Zou: Writing – original draft, Software, Methodology, Investigation, Formal analysis, Data curation. **Xiuru Liang:** Writing – original draft, Investigation, Formal analysis, Data curation. **Wangjuan Dai:** Writing – review & editing, Visualization, Methodology, Investigation. **Ting Zhu:** Validation, Supervision, Software, Resources. **Yutian Zhou:** Visualization, Supervision, Software, Resources, Methodology, Formal analysis. **Yi Qian:** Supervision, Methodology, Data curation, Conceptualization. **Zhengjie Yan:** Software, Methodology, Investigation. **Chao Gao:** Validation, Supervision, Software, Methodology, Formal analysis, Data curation, Conceptualization. **Li Gao:** Supervision, Software, Methodology, Investigation, Data curation. **Yugui Cui:** Visualization, Validation, Supervision, Resources, Methodology, Data curation, Conceptualization. **Jiayin Liu:** Supervision, Resources, Project administration, Funding acquisition, Conceptualization. **Yan Meng:** Writing – review & editing, Visualization, Validation, Supervision, Resources, Project administration, Methodology, Investigation, Funding acquisition, Formal analysis, Data curation, Conceptualization.

Declaration of competing interest

The authors declare that they have no known competing financial interests or personal relationships that could have appeared to influence the work reported in this paper.

Data availability

The data supporting the findings from this study are available within the article file and its supplementary information.

Acknowledgements

Not applicable.

Appendix A. Supplementary data

Supplementary data to this article can be found online at https://doi.org/10.1016/j.bbadis.2024.167334.

References

[1] E. Gershon, N. Dekel, Newly identified regulators of ovarian Folliculogenesis and ovulation, Int. J. Mol. Sci. 21 (2020).
[2] J.L. Tilly, D.A. Sinclair, Germline energetics, aging, and female infertility, Cell Metab. 17 (2013) 838–850.
[3] A. Perheentupa, I. Huhtaniemi, Aging of the human ovary and testis, Mol. Cell. Endocrinol. 299 (2009) 2–13.
[4] F. Timoteo-Ferreira, D. Abreu, S. Mendes, L. Matos, A.R. Rodrigues, H. Almeida, E. Silva, Redox imbalance in age-related ovarian dysfunction and perspectives for its prevention, Ageing Res. Rev. 68 (2021) 101345.
[5] S. Zhang, D. Zhu, X. Mei, Z. Li, J. Li, M. Xie, H.J.W. Xie, S. Wang, K. Cheng, Advances in biomaterials and regenerative medicine for primary ovarian insufficiency therapy, Bioact Mater 6 (2021) 1957–1972.
[6] J. Tesarik, M. Galan-Lazaro, R. Mendoza-Tesarik, Ovarian aging: molecular mechanisms and medical management, Int. J. Mol. Sci. 22 (2021).

[7] C. Tatone, F. Amicarelli, The aging ovary–the poor granulosa cells, Fertil. Steril. 99 (2013) 12–17.
[8] I. Carvacho, M. Piesche, T.J. Maier, K. Machaca, Ion Channel function during oocyte maturation and fertilization, Front. Cell Dev. Biol. 6 (2018) 63.
[9] L. Secomandi, M. Borghesan, M. Velarde, M. Demaria, The role of cellular senescence in female reproductive aging and the potential for senotherapeutic interventions, Hum. Reprod. Update 28 (2022) 172–189.
[10] M. Ozols, A. Eckersley, K.T. Mellody, V. Mallikarjun, S. Warwood, R. O'Cualain, D. Knight, R.E.B. Watson, C.E.M. Griffiths, J. Swift, M.J. Sherratt, Peptide location fingerprinting reveals modification-associated biomarker candidates of ageing in human tissue proteomes, Aging Cell 20 (2021) e13355.
[11] C. Lopez-Otin, M.A. Blasco, L. Partridge, M. Serrano, G. Kroemer, The hallmarks of aging, Cell 153 (2013) 1194–1217.
[12] S. Kaushik, A.M. Cuervo, Proteostasis and aging, Nat. Med. 21 (2015) 1406–1415.
[13] J. Fujii, Y. Ikeda, T. Kurahashi, T. Homma, Physiological and pathological views of peroxiredoxin 4, Free Radic. Biol. Med. 83 (2015) 373–379.
[14] Y. Qian, L. Shao, C. Yuan, C.Y. Jiang, J. Liu, C. Gao, L. Gao, Y.G. Cui, S.W. Jiang, J. Y. Liu, Y. Meng, Implication of differential Peroxiredoxin 4 expression with age in ovaries of mouse and human for ovarian aging, Curr. Mol. Med. 16 (2016) 243–251.
[15] X. Liang, Z. Yan, W. Ma, Y. Qian, X. Zou, Y. Cui, J. Liu, Y. Meng, Peroxiredoxin 4 protects against ovarian ageing by ameliorating D-galactose-induced oxidative damage in mice, Cell Death Dis. 11 (2020) 1053.
[16] S. Wang, Y. Zheng, J. Li, Y. Yu, W. Zhang, M. Song, Z. Liu, Z. Min, H. Hu, Y. Jing, X. He, L. Sun, L. Ma, C.R. Esteban, P. Chan, J. Qiao, Q. Zhou, J.C. Izpisua Belmonte, J. Qu, F. Tang, G.H. Liu, Single-cell transcriptomic atlas of primate ovarian aging, Cell 180 (2020) 585–600 e519.
[17] E. Zito, PRDX4, an endoplasmic reticulum-localized peroxiredoxin at the crossroads between enzymatic oxidative protein folding and nonenzymatic protein oxidation, Antioxid. Redox Signal. 18 (2013) 1666–1674.
[18] E. Zito, E.P. Melo, Y. Yang, A. Wahlander, T.A. Neubert, D. Ron, Oxidative protein folding by an endoplasmic reticulum-localized peroxiredoxin, Mol. Cell 40 (2010) 787–797.
[19] U.T. Phan, R.L. Lackman, P. Cresswell, Role of the C-terminal propeptide in the activity and maturation of gamma -interferon-inducible lysosomal thiol reductase (GILT), Proc. Natl. Acad. Sci. U. S. A. 99 (2002) 12298–12303.
[20] M. Rezaei-Moshaei, A. Bandehagh, A. Dehestani, A. Pakdin-Parizi, M. Golkar, Molecular cloning and in-depth bioinformatics analysis of type II ribosome-inactivating protein isolated from Sambucus ebulus, Saudi, Aust. J. Biol. Sci. 27 (2020) 1609–1623.
[21] I. Mehmeti, S. Lortz, M. Elsner, S. Lenzen, Peroxiredoxin 4 improves insulin biosynthesis and glucose-induced insulin secretion in insulin-secreting INS-1E cells, J. Biol. Chem. 289 (2014) 26904–26913.
[22] M. Bertolotti, S.H. Yim, J.M. Garcia-Manteiga, S. Masciarelli, Y.J. Kim, M.H. Kang, Y. Iuchi, J. Fujii, R. Vene, A. Rubartelli, S.G. Rhee, R. Sitia, B- to plasma-cell terminal differentiation entails oxidative stress and profound reshaping of the antioxidant responses, Antioxid. Redox Signal. 13 (2010) 1133–1144.
[23] E. Zito, H.G. Hansen, G.S. Yeo, J. Fujii, D. Ron, Endoplasmic reticulum thiol oxidase deficiency leads to ascorbic acid depletion and noncanonical scurvy in mice, Mol. Cell 48 (2012) 39–51.
[24] C. Hetz, K. Zhang, R.J. Kaufman, Mechanisms, regulation and functions of the unfolded protein response, Nat. Rev. Mol. Cell Biol. 21 (2020) 421–438.
[25] Y. Qin, X. Jiao, J.L. Simpson, Z.J. Chen, Genetics of primary ovarian insufficiency: new developments and opportunities, Hum. Reprod. Update 21 (2015) 787–808.
[26] Q.R. Fan, W.A. Hendrickson, Structure of human follicle-stimulating hormone in complex with its receptor, Nature 433 (2005) 269–277.
[27] X. Jiang, D. Fischer, X. Chen, S.D. McKenna, H. Liu, V. Sriraman, H.N. Yu, A. Goutopoulos, S. Arkinstall, X. He, Evidence for follicle-stimulating hormone receptor as a functional trimer, J. Biol. Chem. 289 (2014) 14273–14282.
[28] X. Jiang, H. Liu, X. Chen, P.H. Chen, D. Fischer, V. Sriraman, H.N. Yu, S. Arkinstall, X. He, Structure of follicle-stimulating hormone in complex with the entire ectodomain of its receptor, Proc. Natl. Acad. Sci. U. S. A. 109 (2012) 12491–12496.
[29] J. Duan, P. Xu, H. Zhang, X. Luan, J. Yang, X. He, C. Mao, D.D. Shen, Y. Ji, X. Cheng, H. Jiang, Y. Jiang, S. Zhang, Y. Zhang, H.E. Xu, Mechanism of hormone and allosteric agonist mediated activation of follicle stimulating hormone receptor, Nat. Commun. 14 (2023) 519.
[30] Q. Yi, C. Meng, L.B. Cai, Y.G. Cui, J.Y. Liu, Y. Meng, Peroxiredoxin 4, a new oxidative stress marker in follicular fluid, may predict in vitro fertilization and embryo transfer outcomes, Ann Transl Med 8 (2020) 1049.
[31] J. Hwang, L. Qi, Quality control in the endoplasmic reticulum: crosstalk between ERAD and UPR pathways, Trends Biochem. Sci. 43 (2018) 593–605.
[32] Y. Qian, X. Zou, X. Liang, N. Lu, Y. Cui, J. Liu, Y. Meng, Peroxiredoxin 4, a new favorable regulator, can protect oocytes against oxidative stress damage during in vitro maturation, Biochem. Biophys. Res. Commun. 601 (2022) 52–58.
[33] W. Paschen, Dependence of vital cell function on endoplasmic reticulum calcium levels: implications for the mechanisms underlying neuronal cell injury in different pathological states, Cell Calcium 29 (2001) 1–11.
[34] Y. Nishi, T. Yanase, Y. Mu, K. Oba, I. Ichino, M. Saito, M. Nomura, C. Mukasa, T. Okabe, K. Goto, R. Takayanagi, Y. Kashimura, M. Haji, H. Nawata, Establishment and characterization of a steroidogenic human granulosa-like tumor cell line, KGN, that expresses functional follicle-stimulating hormone receptor, Endocrinology 142 (2001) 437–445.
[35] Y. Iuchi, F. Okada, S. Tsunoda, N. Kibe, N. Shirasawa, M. Ikawa, M. Okabe, Y. Ikeda, J. Fujii, Peroxiredoxin 4 knockout results in elevated spermatogenic cell death via oxidative stress, Biochem. J. 419 (2009) 149–158.
[36] P. Chen, W. Li, X. Liu, Y. Wang, H. Mai, R. Huang, Circular RNA expression profiles of ovarian granulosa cells in advanced-age women explain new mechanisms of ovarian aging, Epigenomics 14 (2022) 1029–1038.
[37] A. Salminen, K. Kaarniranta, ER stress and hormetic regulation of the aging process, Ageing Res. Rev. 9 (2010) 211–217.
[38] T.J. Tavender, N.J. Bulleid, Peroxiredoxin IV protects cells from oxidative stress by removing H2O2 produced during disulphide formation, J. Cell Sci. 123 (2010) 2672–2679.
[39] Y. Meng, Y. Qian, L. Gao, L.B. Cai, Y.G. Cui, J.Y. Liu, Downregulated expression of peroxiredoxin 4 in granulosa cells from polycystic ovary syndrome, PloS One 8 (2013) e76460.
[40] R. Diaz Brinton, Minireview: translational animal models of human menopause: challenges and emerging opportunities, Endocrinology 153 (2012) 3571–3578.
[41] B. Zhang, X. Li, G. Liu, C. Zhang, X. Zhang, Q. Shen, G. Sun, X. Sun, Peroxiredomin-4 ameliorates lipotoxicity-induced oxidative stress and apoptosis in diabetic cardiomyopathy, Biomed. Pharmacother. 141 (2021) 111780.
[42] Z. Rao, S. Wang, J. Wang, Peroxiredoxin 4 inhibits IL-1beta-induced chondrocyte apoptosis via PI3K/AKT signaling, Biomed. Pharmacother. 90 (2017) 414–420.
[43] N. Huang, Y. Yu, J. Qiao, Dual role for the unfolded protein response in the ovary: adaption and apoptosis, Protein Cell 8 (2017) 14–24.
[44] R.C. Taylor, A. Dillin, Aging as an event of proteostasis collapse, Cold Spring Harb. Perspect. Biol. 3 (2011).
[45] E. Zito, K.T. Chin, J. Blais, H.P. Harding, D. Ron, ERO1-beta, a pancreas-specific disulfide oxidase, promotes insulin biogenesis and glucose homeostasis, J. Cell Biol. 188 (2010) 821–832.
[46] T. Takagi, T. Homma, J. Fujii, N. Shirasawa, H. Yoriki, Y. Hotta, Y. Higashimura, K. Mizushima, Y. Hirai, K. Katada, K. Uchiyama, Y. Naito, Y. Itoh, Elevated ER stress exacerbates dextran sulfate sodium-induced colitis in PRDX4-knockout mice, Free Radic. Biol. Med. 134 (2019) 153–164.
[47] K. Aittomaki, J.L. Lucena, P. Pakarinen, P. Sistonen, J. Tapanainen, J. Gromoll, R. Kaskikari, E.M. Sankila, H. Lehvaslaiho, A.R. Engel, E. Nieschlag, I. Huhtaniemi, A. de la Chapelle, Mutation in the follicle-stimulating hormone receptor gene causes hereditary hypergonadotropic ovarian failure, Cell 82 (1995) 959–968.
[48] C.A. Kelton, S.V. Cheng, N.P. Nugent, R.L. Schweickhardt, J.L. Rosenthal, S. A. Overton, G.D. Wands, J.B. Kuzeja, C.A. Luchette, S.C. Chappel, The cloning of the human follicle stimulating hormone receptor and its expression in COS-7, CHO, and Y-1 cells, Mol. Cell. Endocrinol. 89 (1992) 141–151.
[49] I. Beau, P. Touraine, G. Meduri, A. Gougeon, A. Desroches, C. Matuchansky, E. Milgrom, F. Kuttenn, M. Misrahi, A novel phenotype related to partial loss of function mutations of the follicle stimulating hormone receptor, J. Clin. Invest. 102 (1998) 1352–1359.
[50] J. Llewellyn, S.J. Hubbard, J. Swift, Translation is an emerging constraint on protein homeostasis in ageing, Trends Cell Biol. (2024). S0962-8924(24)00024-2, https://doi.org/10.1016/j.tcb.2024.02.001. Epub ahead of print. PMID:38423854.
[51] A. Meller, R. Shalgi, The aging proteostasis decline: from nematode to human, Exp. Cell Res. 399 (2021) 112474.
[52] C. Hetz, E. Chevet, H.P. Harding, Targeting the unfolded protein response in disease, Nat. Rev. Drug Discov. 12 (2013) 703–719.
[53] D.J. Maly, F.R. Papa, Druggable sensors of the unfolded protein response, Nat. Chem. Biol. 10 (2014) 892–901.
[54] C.M. Gallagher, P. Walter, Ceapins inhibit ATF6alpha signaling by selectively preventing transport of ATF6alpha to the Golgi apparatus during ER stress, Elife 5 (2016).
[55] C.M. Gallagher, C. Garri, E.L. Cain, K.K.H. Ang, C.G. Wilson, S. Chen, B.R. Hearn, P. Jaishankar, A. Aranda-Diaz, M.R. Arkin, A.R. Renslo, P. Walter, Ceapins are a new class of unfolded protein response inhibitors, selectively targeting the ATF6α branch, Elife 5 (2016).
[56] E. Dufey, D. Sepulveda, D. Rojas-Rivera, C. Hetz, Cellular mechanisms of endoplasmic reticulum stress signaling in health and disease. 1. An overview, Am. J. Physiol. Cell Physiol. 307 (2014) C582–C594.